I.M. BARBOSA[1], E. DEL MORAL HERNANDEZ[2], M.L.C.C. REIS[3], O.A.F. MELLO[4]

[1,2] Universidade de São Paulo, Brasil
e-mail: barbobosa@poli.usp.br
[3,4] Comando-geral de Tecnologia Aeroespacial, São José dos Campos, Brasil

MEASUREMENT UNCERTAINTY CONTRIBUTION TO THE MLP NEURAL NETWORK LEARNING ALGORITHM APPLIED TO AERODYNAMIC EXTERNAL BALANCE CALIBRATION CURVE FITTING

The aim of this study is to fit a calibration curve to a multivariate measurement system considering uncertainty in load measurements. The experimental data are generated from the calibration of the aerodynamic external balance of the subsonic wind tunnel n.º 2, at the Brazilian Institute of Aeronautics and Space. To fit the calibration curve, Multilayer Perceptron Artificial Neural Networks are submitted to the learning process. Studies employing several different architectures were carried out in order to improve the MLP convergence. The uncertainty in measurements is taken into consideration, through the modification of the learning algorithm, which in its classical approach, considers the data points free from error sources. The results of both methodologies, learning algorithm endowed with and without uncertainties, are compared. The artificial neural network performance in predicting future calibration data is explored through the simulation process.

Keywords: Multilayer Perceptrons Artificial Neural Network, calibration curve fitting, uncertainty in measurements, external aerodynamic balance, wind tunnel tests

1. INTRODUCTION

In modern metrology there is great concern about uncertainty. The international references, the ISO/IEC 17025 [1] and the ISO GUM [2] recommend the assessment of uncertainty in measurements. In general aspects, calibrations are performed in order to maintain the measurement traceability. It is worth emphasizing the important role of uncertainty in the traceability definition [3]: "property of the result of a measurement or the value of a standard whereby it can be related to stated references, usually national or international standards, through an unbroken chain of comparisons, all having stated uncertainties".

The calibration curve establishes the relationship between the input and output quantities. This relationship is sometimes nonlinear. In the case of the external balance at the subsonic wind tunnel n.º 2, TA-2, the calibration curve relates the load cell readings to the loads applied to the balance during calibration. The quantity of the load cell readings is the difference of electrical potential and the quantities of the loads are force or moments of force. The loading is performed by applying weights through a system of cables and pulleys [4, 5].

The learning process of an Artificial Neural Network (ANN) was chosen, from one of the several approaches available, to perform the multivariate curve fitting to the external balance calibration data set. The Multi Layer Perceptrons (MLPs) was the class of ANN employed.

In the learning process of the MLP, it is unusual to consider the uncertainties in the output values. The subject of the present work is the development of a methodology for modifying the MLP learning algorithm, taking into consideration the uncertainties in the output values.

A simulation mode is performed in order to verify the repeatability of the external balance calibration.

2. THE EXTERNAL BALANCE CALIBRATION

A six component external balance is used to measure the loads F_i (i = 1, …, 6) acting on the model during the wind tunnel test at the TA-2 aerodynamic facility (Fig. 1).

A balance calibration is performed prior to the tests [4]. The calibration is accomplished by applying loads to the calibration cross through a system of cables and pulleys (Fig. 2). A set of approximately one hundred 10 kg weights is used.

The symbols F_1, F_2, F_3, F_4, F_5, and F_6 are used for the drag, side and lift forces, and the rolling, pitching and yawing moments, respectively. The load cells of the balance provide the readings S_i (i = 1, …, 6).

At the subsonic wind tunnel TA-2, a calibration performed at $\beta = 0$ (Sideslip angle) is called *alpha* calibration and *beta* calibration when otherwise. Seventy three and two hundred and nineteen loading combinations are employed for alpha and beta calibrations, respectively. Table 1 presents some typical loading combinations.

Two alpha calibrations presenting the same configuration are used in this study. The first one is employed in the MLP learning process and the other to verify the repeatability.

Fig. 1. The TA-2 external aerodynamic balance.

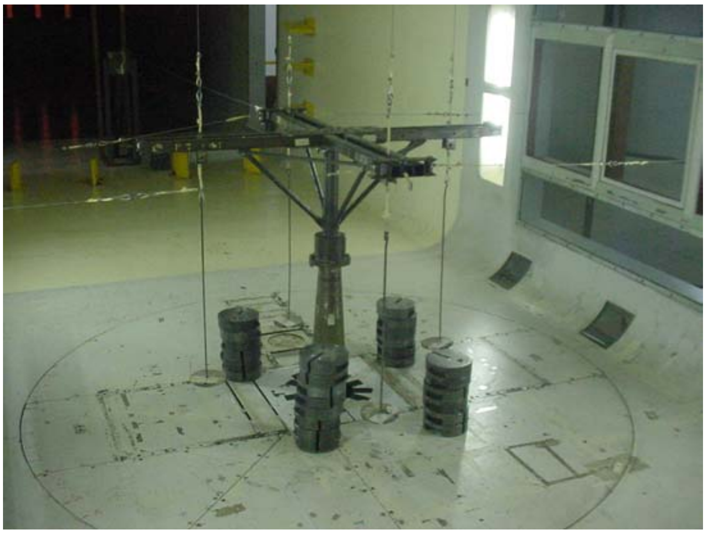

Fig. 2. Loading system for the balance calibration.

Table 1: Some typical balance calibration loadings. Unit: newton for force and newton×meter for moments.

Aerodynamic loads	Loading number				
	1	*26*	*38*	*50*	*71*
F_1	0	100	0	0	200
F_2	0	0	300	-300	0
F_3	-400	0	0	0	400
F_4	0	-100	0	100	0
F_5	-100	0	0	0	0
F_6	0	0	120	0	0

3. THE MULTILAYER PERCEPTRONS ARTIFICIAL NEURAL NETWORK

Artificial Neural Networks are computational intelligence techniques, which may be considered capable of resolving certain classes of problems, among them the approximation of functions, sometimes called mathematical modeling. The approximation of the function may be used to fit the calibration curve taking into account the quantities related to the calibration process. The kind of artificial network employed is the Multilayer Perceptrons (MLP). Neural Networks have already been used in calibration curve fittings [6].

A node may represent the artificial neuron, based on the biological neuron. The node has a single output and several inputs. Each input signal is multiplied individually by a factor called synaptic weight. One of the inputs is chosen as being equal to 1 (threshold). The results of this operation are summed, which is called the weighted sum. The weighted sum is the input value of the transfer function.

Figure 3 presents the architectural graph of the artificial neural network used in this study. It has an input layer of source nodes, a hidden neuron layer and an output neuron layer. It is referred to as multilayer perceptrons and is said to be fully connected, as every node in each layer of the network is connected to every other node in the adjacent forward layer.

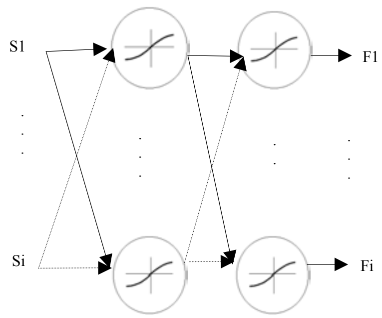

Fig. 3. MLP neural network architectural graph.

There are two modes of MLP operation, the learning process and the simulation process. In the former, the desired input/output vector pairs are supplied to the source/output nodes of the MLP. Adjustments are applied to the synaptic weights *W* through the iterative learning process. The suitable values of the synaptic weights are those that decrease the index performance, known as Performance Function (PF). In the latter form of network operation, the input vectors obtained during testing are supplied to the source layer of the MLP and from the weights *W* fixed during the learning phase one obtains the values of the corresponding output vectors [7].

The conception of the MLP involves the following aspects:

– Number of layers. In this work, it is equal to three;

– Number of neurons in each layer. The hidden layers may have any number of neurons. The number of output variables limits the number of neurons of the output layer. In this study several three-layered MLP are employed, where the number of neurons of the hidden layer and the number of the nodes of the source layer change;
– Transfer Function (TF). It is based on the biological neuron transfer function: the sigmoid function. Equation (1) expresses the TF employed in this study

$$\varphi = \frac{2}{\left[1+\exp(-2x)\right]} - 1, \tag{1}$$

– Learning algorithm. The learning algorithm used is the Levemberg-Maquardt method [8]. The algorithm was modified to account for the uncertainties in the MLP output;
– Synaptic weights initialization. This parameter determines the convergence and the period of convergence of the neural network. For initialization, the value of the synaptic weights chosen is 0.0001;
– Learning performance or Performance Function (PF). The measure of learning performance is the quadratic error summation, Σe^2, which consists of the squared difference between the actual response of the neural network and the desired response, summed over the entire data set. There are several other PFs that can be used based on the quadratic error summation, such as the Mean Square Error (MSE) [7]:

$$MSE = \sqrt{\frac{\sum (e^2)}{\ell}}, \tag{2}$$

ℓ being the number of elements of entire data set ($\ell = 73 \times 6 = 438$);
– Learning rate. A suitable choice of this rate avoids the trapping of the artificial neural network in the local minimum. The algorithm tries several rates for the MLP convergence. The step chosen for the learning rate increment is equal to 50;
– Iterative number. It leads to an improvement of the PF. Each iteration corresponds to the presentation of the complete set of input/output vectors pairs to the artificial neural network. In this study, this number is 2000.

In mathematical terms, the neurons of the MLP for each output variable F_i are described by the following equation:

$$F_i = \varphi_i\left(\sum_{n=1}^{N} w_{2in}\varphi_n\left(\sum_{m=1}^{M} w_{1nm}S_m\right)\right), \tag{3}$$

$n = 1, 2, \ldots, \ldots N$ is the hidden layer neuron index,
$m = 1, 2, \ldots, \ldots M$ is the source layer node index,
φ_i - transfer function of the neurons of the output layer,
W_{2in} - synaptic weights of the neurons of the output layer,
φ_n - transfer function of the neurons of the hidden layer,
W_{1in} - synaptic weights of the neurons of the hidden layer,
S_m are the input signals.

The MLP synaptic weights are set through the Levemberg-Maquardt learning process. This process consists of a regression based on least squares, with a linear approach around the error points at the n^{th} iteration [6]. The synaptic weights are set through the matrix equation:

$$\vec{w}(n+1) = \vec{w}(n) - \left[\vec{J}^T(n)\vec{J}(n) + \lambda\vec{I}\right]^{-1}\vec{J}^T(n)\vec{e}(n), \tag{4}$$

n - 1, 2,… iteration index,
$\vec{w}$ - column vector of synaptic weights and thresholds,
$\vec{e}$ - column vector of output errors (difference between the desired and MLP output values);
$\vec{J}$ - Jacobean matrix, expressed by Eq. (5).

$$\vec{J}(n) = \begin{bmatrix} \partial e1/\partial w1 & \cdots & \partial e1/\partial wm \\ . & . & . \\ . & . & . \\ \partial en/\partial w1 & \cdots & \partial en/\partial wm \end{bmatrix}. \tag{5}$$

Following the traceability definition and the metrological recommendations [1, 2], data uncertainties were considered in the MLP learning algorithm.

The steps for modifying the learning algorithm for best metrology practice involve first-order Taylor series approximation of the error vector around the n^{th} iteration:

$$\vec{e}(n+1,\vec{w}) = \vec{e}(n) + \vec{J}(n)[\vec{w}(n+1) - \vec{w}(n)]. \tag{6}$$

Minimizing the quadratic error summation considering the uncertainties (covariance matrix) is equivalent to minimizing the expression [8, 9]:

$$\vec{e}^{\,T}(u_F^2)^{-1}\vec{e}, \tag{7}$$

u_F^2 - load covariance matrix.

In this study, just the load variances are considered, i. e., u_F^2 is a diagonal load covariance matrix.

Substituting Eq. (6) into Eq. (7) yields:

$$\{\vec{e}(n) + \vec{J}(n)[\vec{w}(n+1) - \vec{w}(n)]\}^T(u_F^2)^{-1}\{\vec{e}(n) + \vec{J}(n)[\vec{w}(n+1) - \vec{w}(n)]\}. \tag{8}$$

Differentiating Eq. (8) with respect to $\Delta\vec{w} = \vec{w}(n+1) - \vec{w}(n)$, or with respect to $\vec{w}$, and setting the results equal to the null matrix, gives rise to:

$$\vec{J}^{\,T}(n)(u_F^2)^{-1}[\vec{e}(n) + \vec{J}\Delta\vec{w}] = \vec{J}^{\,T}(n)(u_F^2)^{-1}\vec{e}(n) + \vec{J}^{\,T}(n)(u_F^2)^{-1}\vec{J}(n)\Delta\vec{w} = \vec{0}. \tag{9}$$

Rearranging Eq. (9) and inserting the learning rate λ to avoid the singularity of the inverse matrix, one finds the MLP learning equation endowed with uncertainties:

$$\vec{w}(n+1) = \vec{w}(n) - \left[\vec{J}^T(n)(u_F^2)^{-1}\vec{J}(n) + \lambda\vec{I}\right]^{-1}\vec{J}^T(n)(u_F^2)^{-1}\vec{e}(n). \tag{10}$$

4. METHODOLOGY

The methodology of curve fitting through the three-layered MLP consists of submitting it to the learning process for several numbers of neurons in the hidden layer. The learning Performance Functions values were compared either for the entire data set or for the individual load values. Both cases, learning endowed with and without load uncertainties are considered as well.

Besides the first calibration employed in MLP learning, a second one, performed at the same laboratorial configuration, was used to test the short-term calibration repeatability. For the second calibration, the MLP operated in the simulation mode. The input vectors, i.e., the load cell readings, are presented to the MLP source layer. Maintaining the synaptic weights, the output vector values are computed in order to estimate the PFs, which correspond to the quadratic error summation. The PFs were estimated when considering or not considering the load uncertainties.

5. RESULTS AND DISCUSSIONS

Figure 4 presents the uncertainty profile employed in this study, which consists of the uncertainties in the estimation of the friction forces originating between cables and pulleys during the external balance calibration. The average level of the uncertainties is shown as a dotted line.

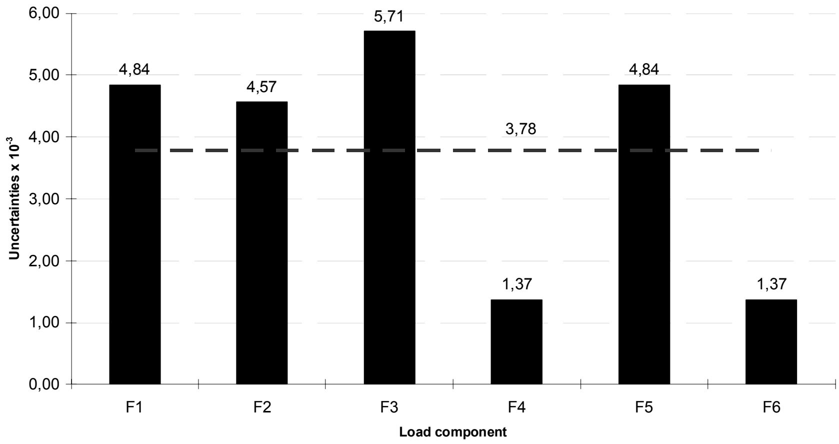

Fig. 4. Load uncertainties and average level. Unit: newton for force and newton×meter for moments.

Figure 5 shows the PF values versus the number of neurons in the hidden layer for the 73 loading configurations. When the number of neurons in the hidden layer increases, there is predominantly a decrease in the PF value. The small graph inserted in the figure emphasizes whether the PF considering the load uncertainties is greater (slower) or less in value (faster) than the PF when not considering them.

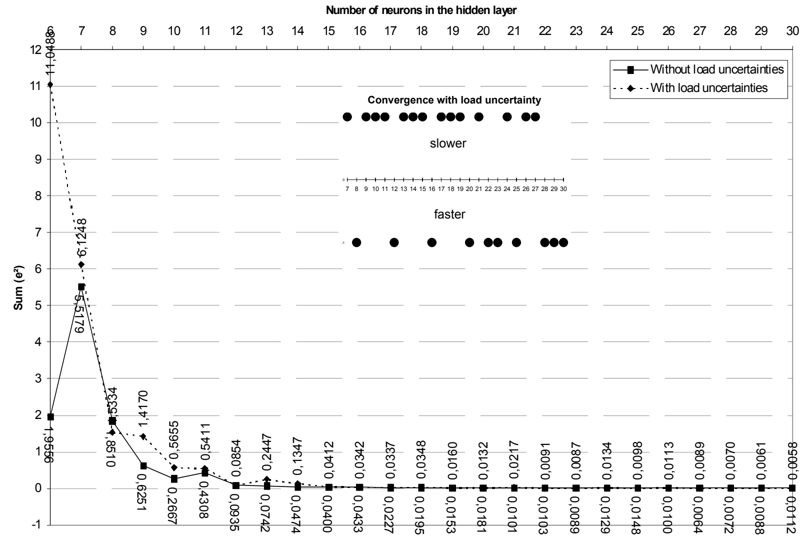

Fig. 5. MLP Performance Function for the learning mode.

The PFs as a function of the number of neurons in the hidden layer, for each load component, are shown in Figs. 6 to 11. The learning algorithm is endowed or not with load uncertainties. These figures highlight the differences between the MLP learning process with and without uncertainties. It can be seen that the quadratic error summation for the loads F_4 and F_6 are predominantly lower for the case without load uncertainties (Figs. 9 and 11). As one can note, this result is in accordance with Fig. 4, which indicates uncertainties associated to loads F_4 and F_6 below the average level. For the other load components either the PFs are higher in the case of considering the uncertainties (Figs. 6, 8, and 10) or the curves intersect each other (Fig. 7). Once again, these results are in accordance with Fig. 4, which presents load uncertainties greater than or close to the average level.

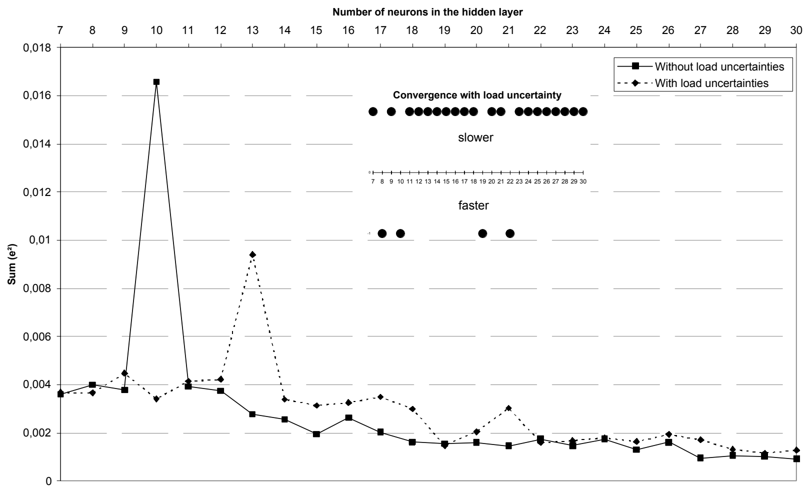

Fig. 6. Learning Mode Performance Functions for F_1.

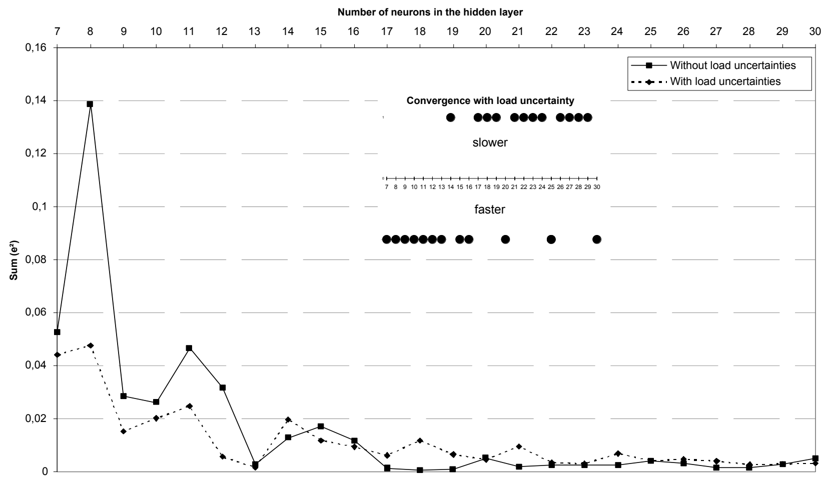

Fig. 7. Learning Mode Performance Functions for F_2.

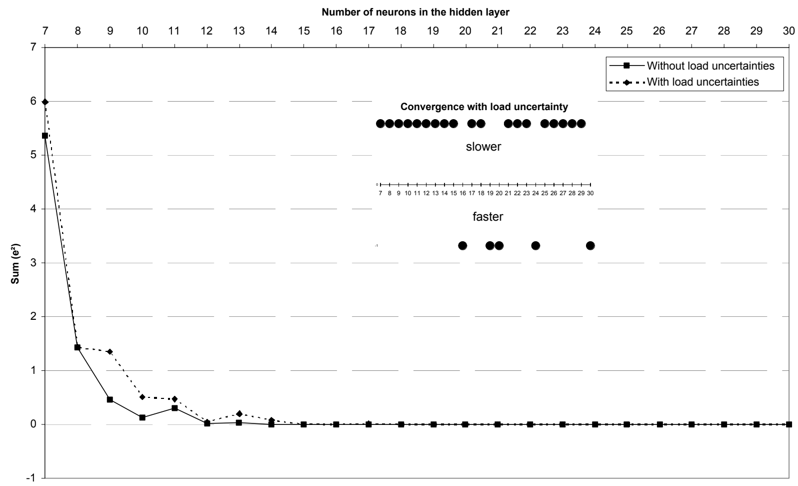

Fig. 8. Learning Mode Performance Functions for F_3.

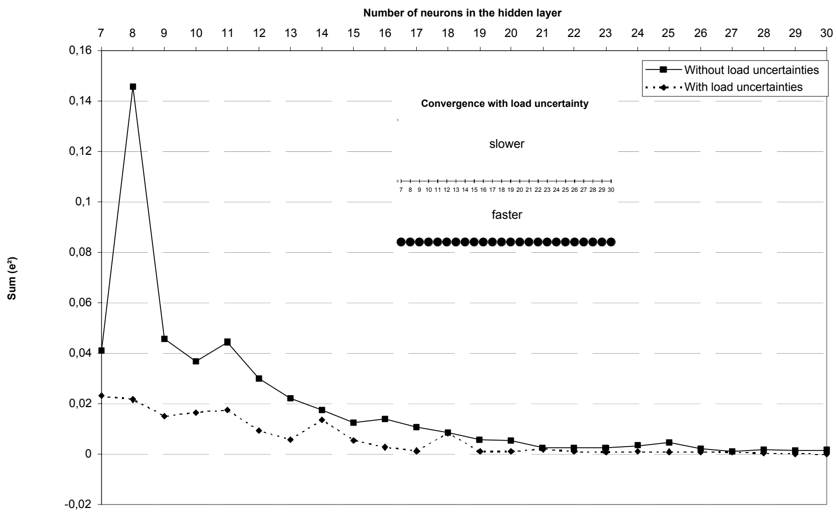

Fig. 9. Learning Mode Performance Functions for F_4.

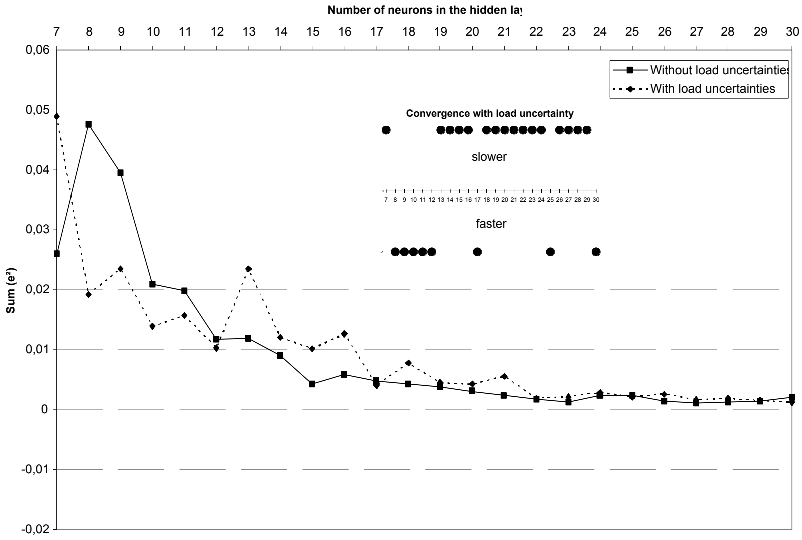

Figure 10. Learning Mode Performance Functions for F_5.

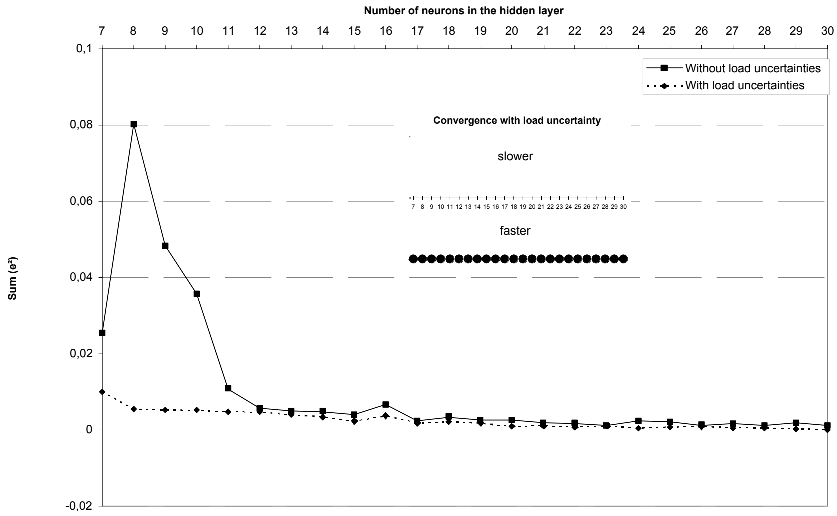

Fig. 11. Learning Mode Performance Functions for F_6.

Figure 12 shows the PFs versus the number of neurons in the hidden layer, for the MLP submitted to the simulation process, with and without considering the load uncertainties. The data from the second calibration were employed. The learning process was performed through the first calibration data, according to Fig. 5. In the PF curves presented, the short-term repeatability of the external balance calibration for the entire data set can be analysed.

One could seek the best MLP architecture to estimate the calibration curve, through the one which promotes the lowest PF value to represent the balance calibration repeatability. Nevertheless, this choice is not so evident, once there is not a defined minimum. Instead, the minimum value oscillates in a region between 6 and 12 neurons in the hidden layer. After this period, a slight tendency for the PF to increase occurs (Fig. 12).

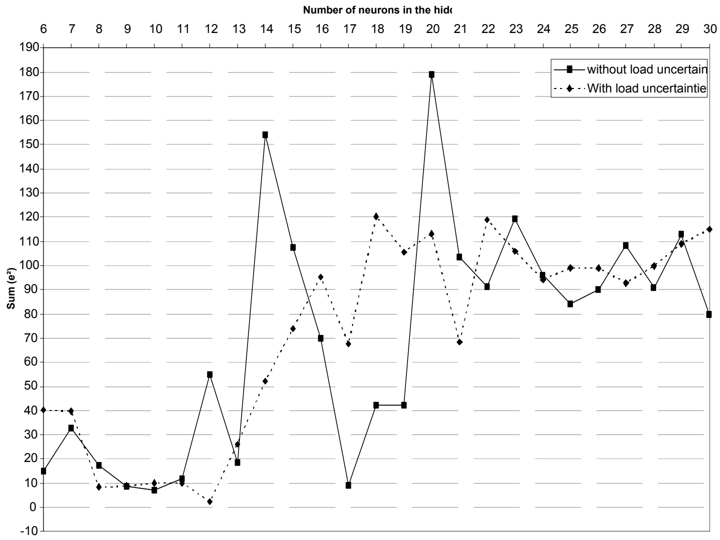

Fig. 12. Performance Functions for the second calibration.

One can use the Mean Square Error (MSE) in order to better visualize this choice. If all the errors of the entire data set had been equal, the MSE would represent each one of these errors [6].

Choosing the MLP architecture that represents the minimum MSE in the learning and simulation process simultaneously could be achieved by the normalization of the MSE per maximum MSE in each process and comparing them.

Figure 13 shows the normalized MSE for the learning and simulation process with and without load uncertainty. If this is the case, one would choose the architectures with 9 to 11 neurons in the hidden layer because the MSE values in the learning and simulation are close.

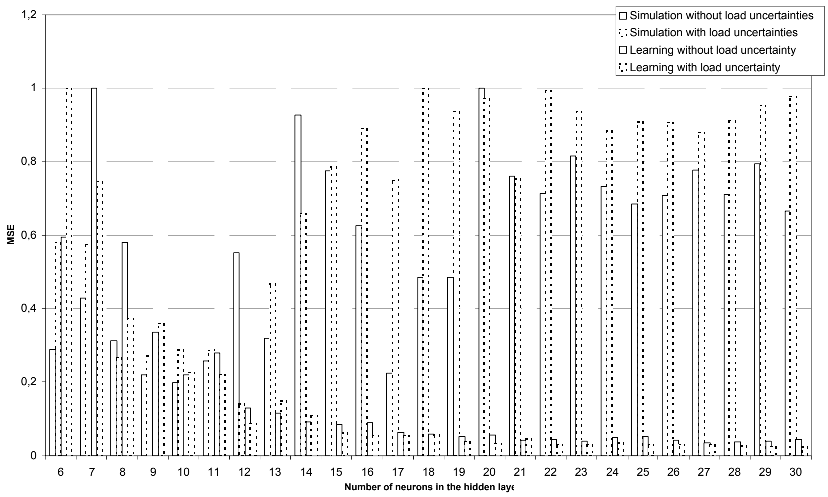

Fig. 13. MSE for the first (learning process) calibration and second (simulation process) calibration with and without load uncertainty.

6. CONCLUSIONS

This study presents a methodology for multivariate curve fitting and for the analysis and maintenance of traceability, related to the data derived from a calibration process.

The MLP Artificial Neural Network was employed to interpolate the calibration data set. Uncertainties in the output quantities were considered in the learning algorithm of the MLP. An analysis of the quadratic error summation convergence due to uncertainties contributions was presented.

With other approaches of uncertainty assessment and calibration there is a necessity of establishing the mathematical relationship between the input and output quantities. However, the MLP has the advantage of solving the relationship between the involved quantities, since the mathematical modeling is the one imposed by the MLP architecture. The drawback is that it is necessary to work on all the aspects cited in section 3.

Calibration curve fitting employing MLP, without considering measurement uncertainties may over- or underestimate the Performance Function, as discussed in section 5.

It is possible to choose the PF accuracy for the calibration curve fitting, employing MLP. The value of the quadratic error summation achieved can be negligible and therefore it is suitable for even the most rigorous measurement accuracy requirements. Obviously, this situation occurs at the expense of computational time, since the processing is iterative and the number of parameters in each layer is proportional to the number of neurons.

One is able to choose a MLP architecture that minimizes both learning and simulation process simultaneously, through the normalized MSE, if required. However, this approach is just an option. The Performance Function may be used to analyse the repeatability of successive calibrations when the MLP is employed in the simulation mode.

The possibility of taking into account the measurement uncertainties, without MLP convergence and computational drawbacks, has been demonstrated. The results agree with the intuition that curve fitting for quantities associated with low uncertainties converges faster. Considering uncertainties is in accordance with metrology best practice, recommended by international standardization [1, 2, 3].

Studies to improve the assessment of the uncertainty in the measured quantities must be carried out. There are several error sources that act during the external balance calibration. Some of them are recognizable and quantifiable, and others may remain unknown. This study considers just the uncertainty in the estimation of the friction forces between cables and pulleys. Contributions from the measurement chain such as data filtering and the process of alignment of the cables in the calibration process are still to be investigated. One should also consider the uncertainties declared in the calibration certificates of the weights applied to the loading system and of the load cells. Besides, just the load variances are considered in the covariance matrix employed in the MLP learning algorithm. The covariances between the aerodynamic loads are still under evaluation. Application of other MLP architectures, with number of layers greater than three, is the next step to be analysed.

7. ACKNOWLEGMENTS

This work was supported by the Foundation for Support of Research of the State of São Paulo (FAPESP) under grant no. 2000/13769-0.

8. REFERENCES

1. ISO/IEC 17025: *General Requirements for the Competence of Testing and Calibration Laboratories*, 2005.
2. ISO: *Guide to the Expression of Uncertainty in Measurement*, 1995.
3. ISO: *International Vocabulary of Basic and General Terms in Metrology*, 1993.
4. Reis M. L. C. C., Vieira W. J., Barbosa I. M., Mello O. A. F., Santos L. A.: *Validation of an External Six-Component Wind Tunnel Balance Calibration*. 24th AIAA Aerodynamic Measurement Technology and Ground Testing Conference, AIAA, Portland, 2004.
5. Reis M. L. C. C., Mello O. A. F., Sadahaki U.: *Calibration Uncertainty of an External Six-Component Wind Tunnel Balance*. 33rd AIAA Fluid Dynamics Conference and Exhibit, AIAA, Florida, 2003.

6. Barbosa I. M.: *Application of the Artificial Neural Networks in Metrological Reliability* (Aplicação das Redes Neurais Artificiais na Confiabilidade Metrológica). Master of Science dissertation, São Paulo, Brasil, 2004.
7. Haykin S. S.: *Neural Network: A Comprehensive Foundation.* 2nd ed., Prentice-Hall, 1999.
8. Lira I.: *Evaluating the Measurement Uncertainty – Fundamental and Practical Guidance*. Institute of Physics Publishing, IOP, 2002.
9. Weise K.: *Treatment of Uncertainties in Precision Measurements Uncertainty*. IEEE Transactions Instrumentation Measurements, vol. IM-36, no. 2, pp. 642-645, 1987.